oC7

PLUME EXPANSION DYNAMICS DURING $Sm_{1-x}Nd_xNiO_3$ THIN FILM DEPOSITION

S. LAFANE, T. KERDJA, S. ABDELLI-MESSACI and S. MALEK
Centre de Développement des Technologies Avancées, Cité 20 août 1956, B.P. 17, Baba Hassen, Algérie
E-mail: slafane@cdta.dz

ABSTRACT: The plume expansion dynamics of an ablated target of Sm_2O_3, Nd_2O_3 and NiO mixture oxides by a KrF excimer laser into oxygen atmosphere has been investigated using fast imaging. The study was carried out for different laser fluences. The plasma plume dynamics was analysed in the framework of the Predtechensky and Mayorov (PM) model. It was found that the PM model gives a general description of the plume expansion from the early time to later time delays by using parameters (laser fluence and oxygen pressure) that ensure a hemispherical expansion of the plume. The latter was discussed in the framework of the shock-wave model.

KEYWORDS: laser ablation, $Sm_{1-x}Nd_xNiO_3$, fast imaging, plume dynamics, Predtechensky and Mayorov model

1. Introduction

Due to its metal–insulator transition and thermochromic properties, the rare earth nickelate perovskite $RNiO_3$ ($R \neq La$), has received a great deal of attention [1].The metal–insulator transition temperature (T_{MI}) can be tuned by changing the R cation. The interesting property is the ability to tune the T_{MI} in the wide range of temperature, especially around the ambient, by adjusting the relative ratio of the cations (R and R') in the $R_{1-x}R'_xNiO_3$ compound [2, 3].
Pulsed laser ablation is used to synthesise a variety of materials such as oxides [4, 5]. The main advantage of this technique is the stoichiometric transfer of the multicomponent target elements to substrate. Nevertheless, in the case of oxides, the deposition under oxygen atmosphere is required to compensate the oxygen loss. The latter is due to the fact that oxygen is a volatile element. Also, it is due to film bombardment by high energetic ablated species where sputtering of the light elements is expected. Thus, the oxygen pressure is used as a moderator for the energetic plume. Therefore, the plume dynamics study is important to control the ejected species energy and consequently the films properties. Elsewhere, a correlation was found between the plume dynamics and the characteristics of the deposited films [6-12].
Several models have been proposed to describe the ablation plume expansion in a background gas. Among these models, shock wave model [13–18] and drag model [14, 19] are widely used in the literature. However, these models fit only a limited region of the experimental data as reported by several authors. Recently, using a simple physical approach proposed by Predtechensky and Mayorov (PM model) [20], Amoruso et al. [21] and Sambri et al. [22–24] showed a good agreement between their experimental data and the prediction of PM model from the early time of the plume expansion until later time delay.
In this work, we study the validity of PM model to describe the plume expansion into oxygen background pressure for three different laser fluences.

2. Experimental

The schematic of the experimental set-up is illustrated in Fig. 1. The vacuum chamber was evacuated first by a turbomolecular pump to a residual pressure of 3×10^{-6} mbar and than filled with oxygen gas. Two cylindrical lenses are used to focus the KrF (λ = 248 nm, τ = 25 ns) laser beam on the rotating target with an incident angle of 45°. The target is a mixture of samarium, neodymium and nickel oxides. The relative ratio of neodymium (x = 0.45) is set to have a T_{MI} close to room temperature (310 K). A set of spherical and planar mirrors and a Zeiss lens (76-mm focal length, spectral response: 350–800 nm) are used to form a two-dimensional image of the luminous plume on the ICCD camera (Princeton Instruments PI-MAX, 1024×256 pixels, pixel size = 26 × 26 µm).The ICCD camera spectral response is within the range of 190–850 nm. The observation was made along the normal to the plume direction of expansion. The study was carried out at 0.2 mbar of oxygen gas pressure. The fluence was fixed at 1.5 and 2 J cm^{-2}. The number of accumulation, ICCD gain and gate are adjusted for each image to compensate the reduction of the plume intensity during the expansion. The target surface and the end of the laser pulse were taken as the origin of distances and time delays.

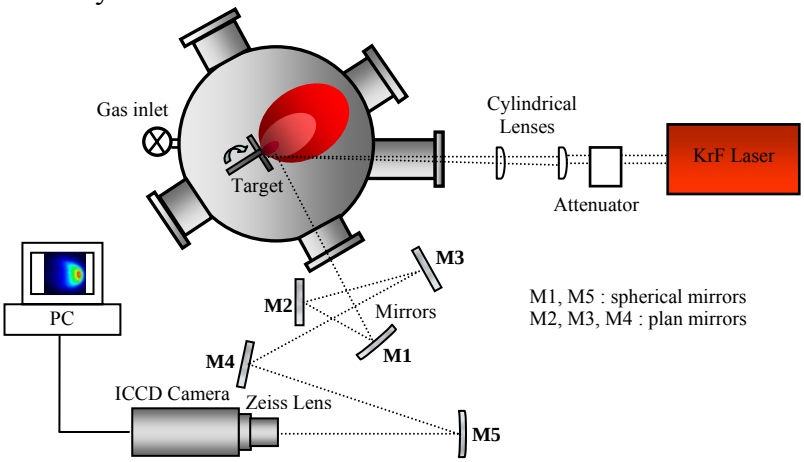

Figure 1: Schematic of the experimental Setup

3. Results and discussion

Typical ICCD images of the temporal evolution of the expanding plume into 0.2 mbar of oxygen pressure and for the two laser fluences used are given in Fig. 2. Each image represents the spectrally integrated emission in the range of 350-800 nm of the plume excited species.

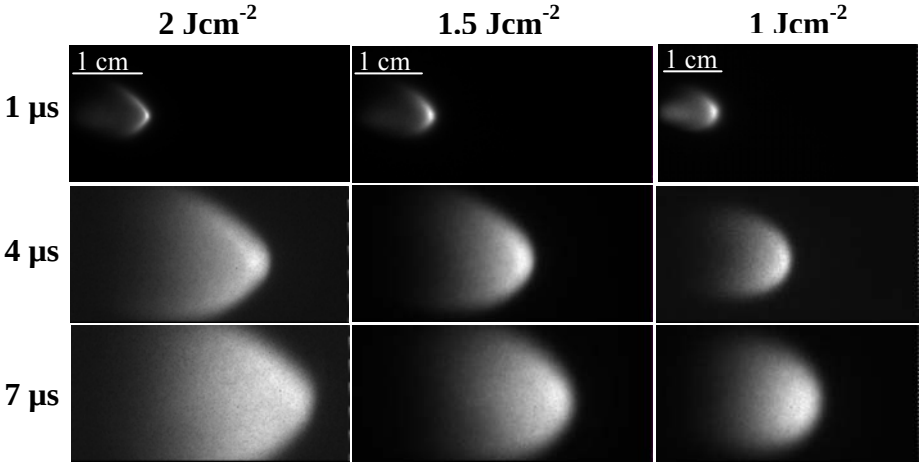

Figure 2: The temporal evolution of the visible plume. The position of the ablating surface is at the limit of the left side of the images.

In order to study the plasma plume expansion dynamics, we plotted the plume luminous front position versus time delay (see Fig. 3). It appears that independently of the laser fluences the plume expansion is still almost linear at early times. The initial plume front velocity passes from 1.7×10^6 cm/s to 1.4×10^6 cm/s when the laser fluence passes from 2 Jcm^{-2} to 1 Jcm^{-2}. As the time evolves a deviation from free-plume expansion occurs and the plume slows down. This effect corresponds to the propagation regime where the ejected species collide with gas molecules and loss their kinetic energy. Later, the plume front comes to rest. This occurs at 3.8 and 3.3 cm for 1.5 and 1 Jcm^{-2} and out of our observation range for 2 Jcm^{-2}. At this stage, the ejected species diffuse into the ambient gas until they reach a distance where they loss completely their kinetic energy. Note that the transition from one expansion regime to the following occurs at different time delays and distances depending on the laser fluence.

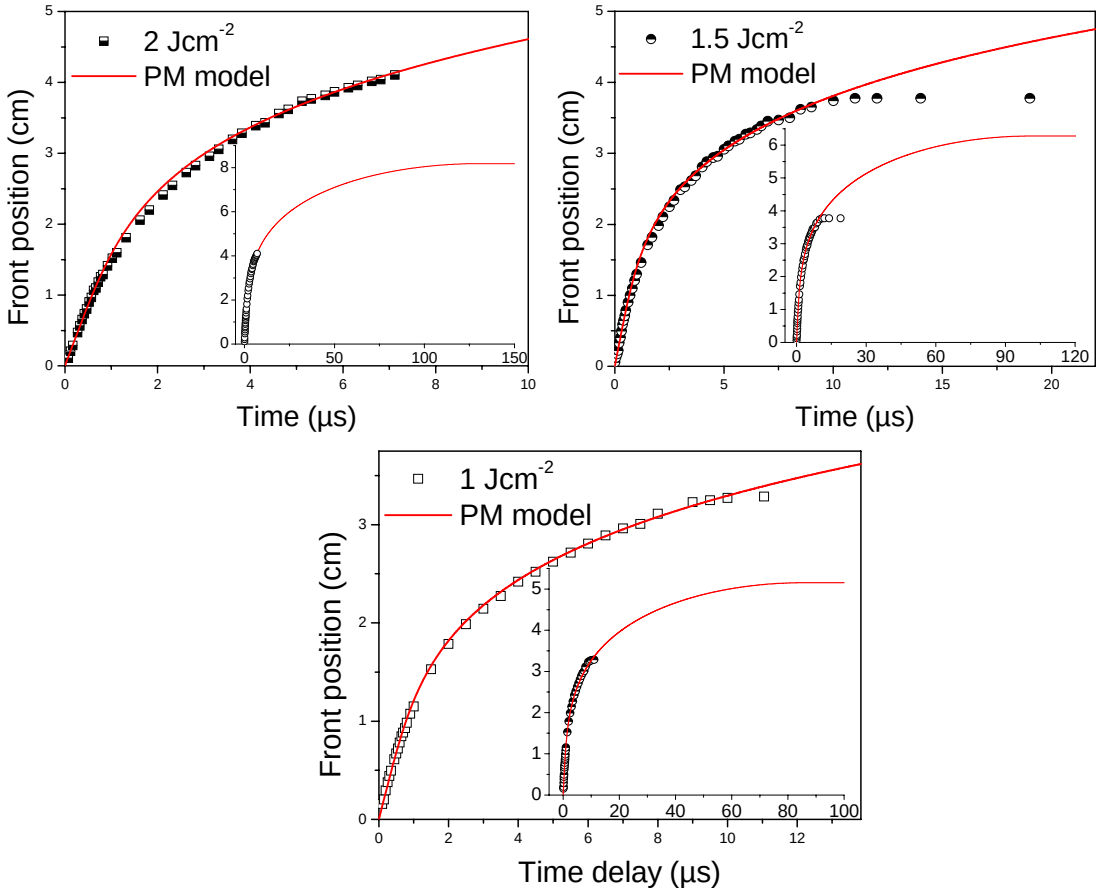

Figure 3: Plume front position as a function of the time delay at fluences of 1.5 and 2 Jcm^{-2} and 0.2 mbar of oxygen pressure. The solid line represents the plume front trajectory predicted by PM model.

The plasma plume dynamics was analysed in the framework of Predtechensky and Mayorov (PM) model. This model is based on the balance between linear momentum variation and the external pressure force. It considers plume and adjoint background gas as a hemispherical thin layer of radius R moving at velocity u and experiencing the force due to the background gas pressure P_0. Then, the equations of motion for R and the velocity u are given as follows [21, 22, 24] :

$$\frac{d}{dt}\left[\left(M_p + M_g(R)\right)u\right] = -2\pi R^2 P_0 \quad (1)$$

$$\frac{dR}{dt} = u(R) \quad (2)$$

where M_p is the confined plume mass. P_0 and $M_g = 2/3\pi\rho_0 R^3$ (ρ_0 being the background gas density) are the background gas, pressure and the swept-up mass. The initial conditions are $R(t = 0) = 0$ and $u(t = 0) = u_0$, u_0 being the initial velocity at the early time of the plume expansion. By changing the variables, $d/dt = u(R)d/dR$, an analytical solution is given to Eqs. (1) and (2) where the front velocity as function of R is given by:

$$u(R) = c_0\sqrt{\frac{b^2}{\left(a^3 + R^3\right)^2} - 1} \quad (3)$$

with

$$a = \sqrt[3]{\frac{3M_p}{2\pi\rho_0}},\ b \approx a^3\left(\frac{u_0}{c_0}\right),\ c_0 = \sqrt{\frac{P_0}{\rho_0}}$$

where a is a characteristic scaling length corresponding to the radial distance from the target at which the mass of the swept-up gas equals the confined plume mass, while b is a constant which depends on the initial conditions. c_0 is a characteristic velocity scaling, which is equal to 278 m/s for the case of oxygen at room temperature. By using the initial plume velocity indicated above and by choosing a suitable value of the plume mass, Eq. (3) has been numerically integrated. The fitted trajectories are shown in Fig. 3 and the predicted parameters (plume, mass and stopping distance) are summarized and compared to the experimental ones in table (I). Note that the experimental plume mass (the ablated one) was obtained by weighing the target before and after irradiation with 6000 laser pulse.

Table 1: Plume stopping distance and mass: comparison between the experimental and PM model predicted ones.

Laser fluence (Jcm^{-2})	Mp(μg) Experimental	Mp (μg) Predicted	R_{st} (cm) Experimental	*R_{st} (cm) Predicted*
1	0.36	0.75	3.2	*5*
1.5	0.75	0.87	3.8	*6.3*
2	*1.13*	*1.1*	*/*	*8*

As we can see on Fig. 3, the predicted trajectory of the plume front agrees well with the major part of our experimental. However, the predicted plume stopping distance is still larger than the experimental one for 1 and 1.5 Jcm^{-2} where the plume stopping is observed. In order to verify if the predicted stopping distance at 2 Jcm^{-2} is also overestimated, a thin layer was deposited onto unheated (100) silicon substrates at this distance (d = 8 cm) for 9000 laser pulses. The obtained layer morphology analysis using Scanning Electron Microscopy revealed a high porous structure (see Fig. 4). This structure is known as a result of a diffusion-like deposition regime where the deposition distance is far from the plume stopping distance [9, 12, 25]. Thus, the stopping distance predicted by PM model is also overestimated at 2 Jcm^{-2}.

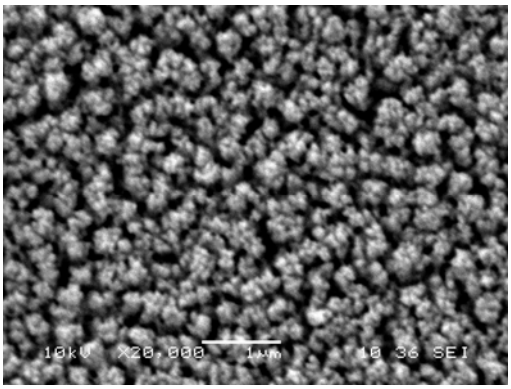

Figure 4: SEM scan of the deposited layer at 2 Jcm^{-2} of laser fluence, 0.2 mbar of oxygen pressure, and 8 cm of target-substrate distance.

The overestimation of the plume stopping distance by PM model could de attributed to the use of the hemispherical expansion simplification. This argument could be supported by considering the predicted to the experimental stopping distance ratio (*r*). In our previous work [27], at 2 Jcm^{-2} and at the pressure used here, the sopping distance was estimated to be around 4.3 cm using drag model. Thus, the ratio (*r*) is 1.55, 1.65 and 1.86 for 1, 1.5 and 2 Jcm^{-2}, respectively. This decreasing of the ratio (*r*) could be correlated to the plume shape. Effectively as we can see on Fig. 2, the latter tends to be less forward-peaked by decreasing the laser fluence.

Concerning the plume mass, as we can on Table 1. the predicted plume mass is very close to the experimental one for 1.5 and 2 Jcm^{-2}. However at 1 Jcm^{-2}, the predicted mass is higher than the experimental one. The overestimation of the plume mass using PM model has already reported by Amoruso et al. [15]. It was attributed to the deviation of the plume expansion from an ideal hemispherical symmetry expansion. However the coincidence of the experimental plume mass with the predicted one at 1.5 and 2 Jcm^{-2} is surprising and further investigation is needed. Also, additional exploration is needed to find the ablation parameters (laser fluence and oxygen pressure) that lead to the hemispherical expansion of the plume and therefore to the study of the validity of PM model in such condition.

4. Conclusion

The expansion dynamics of an ablated plume of Sm_2O_3, Nd_2O_3 and NiO mixture oxides target by KrF laser in background oxygen atmosphere has been investigated using a fast ICCD imaging. The study was done for three laser fluences 1, 1.5 and 2 Jcm^{-2} into 0.2 mbar of oxygen pressure. The plume dynamics was analysed by using Predtechensky and Mayorov (PM) model. It was found that PM model gives a general description of the plume dynamics for all fluences used. However at later time delay, the predicted plume stopping distance was overestimated due to the use of the hemispherical expansion simplification.

References

[1] Galicka K., Szade J., Ruello P., Laffez P. and Ratuszna A.; *Appl. Surf. Sci.* **255** 4355 (2009)

[2] Frand G., Bohnké O., Lacorre P., L. Fourquet J., Carré A., Eid B., Theobald J. G. and Gire A.; *J. Solid State Chem.* **120** 157 (1995)

[3] A. Ambrosini and J.F. Hamet; *Appl. Phys. Lett.* **82** 727 (2003)
[4] Chrisey D.B. and Hubler G.K.; *Pulsed laser deposition of thin films*; John Wiley and Sons, New York (1994)
[5] Bauerle D.; *Laser Processing and Chemistry*; Springer, Berlin (2000)
[6] Gonzalo J., Afonso C.N., Ballestros J.M.; *Appl. Surf. Sci.* **109/110** 606 (1997)
[7] Voevodin A.A., Jones J. G. and Zabinski J. S.; *J. Appl. Phys.* **92** 724 (2002)
[8] Bailini A., Di Fonzo F., Fusi M., Casari C.S., Li Bassi A., Russo V., Baserga A. and Bottani C.E.; *Appl. Sur. Sci.* **253** 8130 (2007)
[9] Dellasega D., Facibeni A., Di Fonzo F., Russo V., Conti C., Ducati C., Casari C.S., Li Bassi A. and Bottani C.E. ; *Appl. Surf. Sci.* **255** 5248 (2009)
[10] Lafane S., Kerdja T., Abdelli-Messaci S., Malek S. and Maaza M. ; *Appl. Surf. Sci.* **256** 1377 (2009)
[11] Riabinina D., Chaker M. and Rosei F.; *Appl. Phys. Lett.* **89** 131501 (2006)
[12] Pereira A., Cultrera L., Dima A., Susu M., Perrone A., Du H.L., Volkov A.O., Cutting R. and Datta P.K. ; *Thin Solid Films* **497** 142 (2006)
[13] Amoruso S., Sambri A. and Wang X.; *J. Appl. Phys.* **100** 013302 (2006)
[14] Harilal S.S., Bindhu C.V., Tillack M.S., Nadjmabadi F. and Gaeris A.C.; *J. Appl. Phys.* **93** 2380 (2002)
[15] Amoruso S., Bruzzesi R., Spinelli N., Velotta R., Vitiello M. and Wang X.; *Phys. Rev. B* **67** 224503 (2003)
[16] Phelps C., Druffner C.J., Perram G.P. and Biggers R.R.; *J. Phys. D: Appl. Phys.* **40** 4447 (2007)
[17] Dyer P.E. and Sidhu J.; *J. Appl. Phys.* **64** 4657 **(**1988)
[18] Amoruso S., Sambri A. and Wang X.; *Appl. Surf. Sci.* **253** 7696 (2007)
[19] D.B. Geohagan, *Thin Solid Film* **220**, 138 (1992)
[20] Predtechensky M.R.and Mayorov A.P.; *Appl. Supercond.* **1** 2011 (1993)
[22] Sambri A., Amoruso S., Wang X., Radovic' M., Granozio F.M.and Bruzzese R.; *Appl. Phys. Lett.* **91** 151501 (2007)
[23] Sambri A., Radovic' M., Wang X., Amoruso S., Miletto Granozio F. and Bruzzese R.; *Appl. Surf. Sci.* ***254*** 790 (2007)
[24] Sambri A., Amoruso S., Wang X., Granozio F.M. and Bruzzese R.; *J. Appl. Phys.* **104** 053304 (2008)
[25] Fusi M., Russo V., Casari C.S., Li Bassi A.and Bottani C.E. ; *Appl. Surf. Sci.* **255** 5334 (2009)
[26] Zeng X., Mao X., wen S.B., Greif R. and Russo R.E.; *J. Phys. D: Appl. Phys.* **37** 1132 (2004)
[27] Lafane S., Kerdja T., Abdelli-Messaci S., Malek S. and M. Maaza; *Appl. Phys. A* **98** 375 (2010)